

# *Improvement of the Quality of Dark Field Images of Electron Microscope with the Increase of Accelerating Voltage*

Toshio SAHASHI

*Department of Physics, Nagoya University, Nagoya*

(Received August 21, 1969)

The dark field images of crystalline objects were taken at accelerating voltages, 50–1000 kV, with the incident beam parallel to the optic axis. Since the image forming ray makes a large angle, twice the Bragg angle, with the optic axis, the image quality is much lower than that of bright field images at ordinary accelerating voltages, 50–100 kV, due to the chromatic and spherical aberrations. It was shown experimentally that in high voltage electron microscopes (higher than 500 kV), both aberrations were much reduced and became almost negligible at 1000 kV for low order reflections.

## § 1. Introduction

In electron microscopy of crystalline objects, there are the bright field images formed by the incident beam and the dark field images formed by a diffracted beam. In many cases, the objects are observed under bright field. By the use of dark field method, the positions where the incident beam is diffracted in a crystalline object can be found, so this method is often used for the study of textures of crystals. For the observation of lattice defects in whiskers<sup>1)</sup> or fine particles the dark field method is indispensable, because the surroundings of objects are too bright under bright field and the inside of the object is not observable. For these reasons, the dark field method is very important in the study of crystalline objects. In the usual dark field method, however, the image-forming ray makes a large angle, twice the Bragg angle, with the optic axis. This results in a large chromatic aberration due to the energy loss of electrons in the specimen and also an apparent astigmatism due to the spherical aberration. In order to avoid these aberrations, the method has been developed in which the incident beam is inclined so that the diffracted one runs along the optic axis. This method, however, is technically complicated and the specimen is often spoiled in the course of the adjustment. It is expected that the chromatic and the spherical aberrations of dark field images become small in high voltage electron microscopes. Therefore, without using the inclination method the dark field images of good quality can

be quickly and easily observed only by moving the objective lens aperture. It is shown experimentally in this paper how the quality of dark field images is improved with the increasing accelerating voltages.

## § 2. Experimental

The specimens used in this experiment were gold particles epitaxially grown on sodium chloride surfaces. They were made as follows.<sup>2)</sup> A small amount of gold (mean thickness about 50 Å) was deposited by the evaporation on cleavage faces of NaCl heated at 400°C in vacuum and then carbon was evaporated. The carbon film with the gold particles was removed from NaCl in water. An example of images and that of diffraction patterns are reproduced in Fig. 1. Typical particles look squares with their sides parallel to  $\langle 110 \rangle$  of NaCl. Judging from the equal thickness contours, the external form of the typical particles is as shown in Fig. 2. The extinction distance for (200) reflection of gold is 180 Å at 100 kV.

The procedure of taking dark field images was as follows: (1) The direction of the incident beam was adjusted so that the bright field image did not shift by adding a small ripple to the accelerating voltage. (2) The astigmatism of the objective lens was corrected by the stigmator under the bright field. (3) The dark field images of four (200) reflections were taken by moving the objective lens aperture onto each Bragg spot without changing the direction of the incident beam. Streaks appeared in dark field images as shown in Fig. 3. They are due

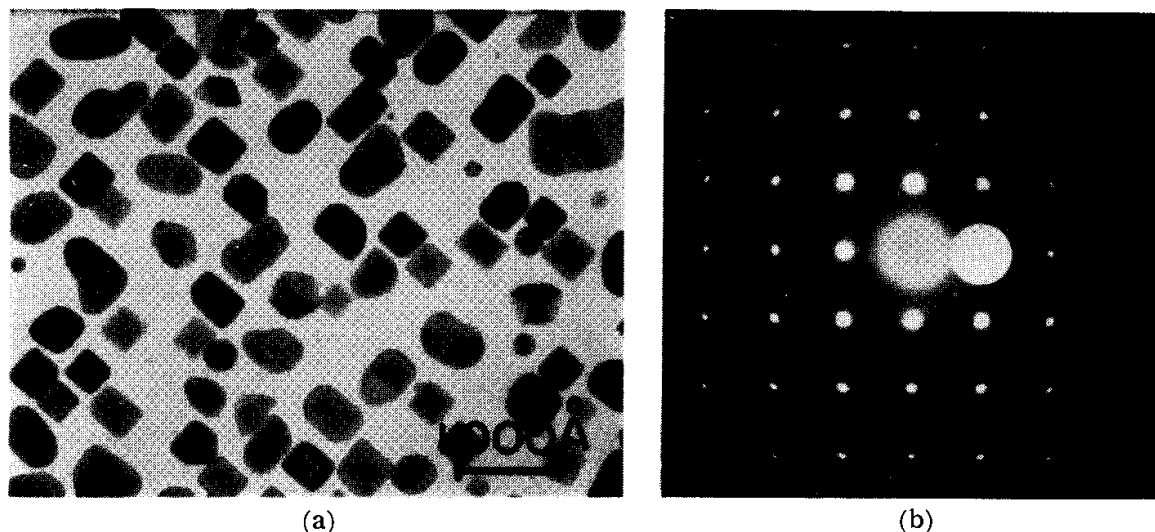


Fig. 1. (a) Bright field image at 800 kV. (b) Diffraction pattern at 500 kV. The white disc is a objective lens aperture at (200) Bragg spot.

to the energy loss of electrons. It was confirmed that the streaks were symmetric as to four {200}. This proves that the incident beam runs exactly along the optic axis of the microscope. The dark field images

of high order reflections {220}, {400}, {440}, etc., were also taken. The direction of the streaks is parallel to the reciprocal lattice vector of the reflecting plane. Thus, in images taken with {200}, {400}, etc., the direction is along the diagonal of the typical particles as seen in Fig. 3 and in {220}, {440},

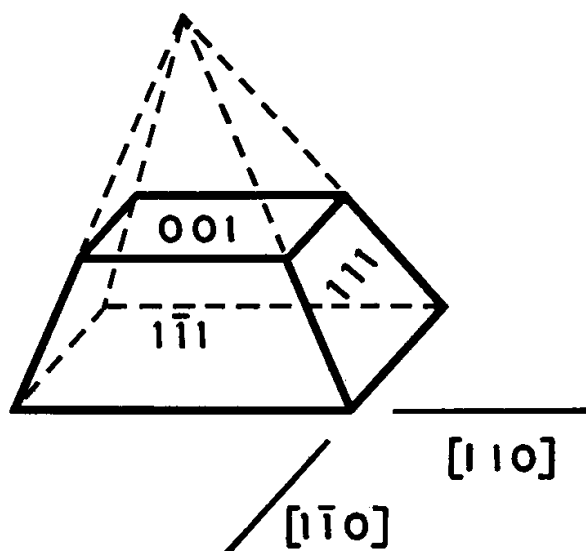


Fig. 2. External form of a typical particle.



Fig. 3. Dark field image at 50 kV, (200) reflection.

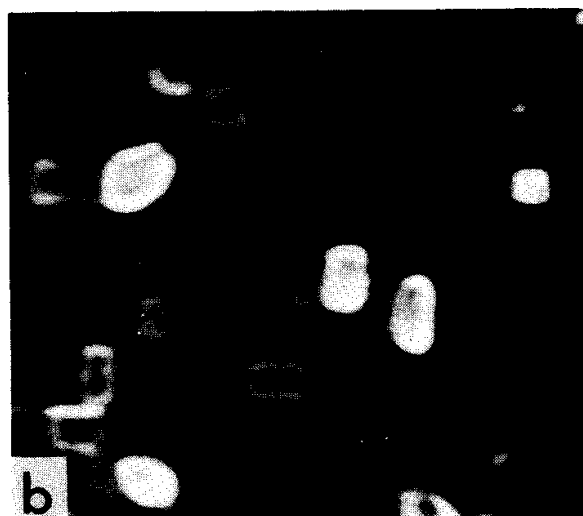


Fig. 4. Dark field images at 100 kV. (a) (200) reflection. (b) (220) reflection.

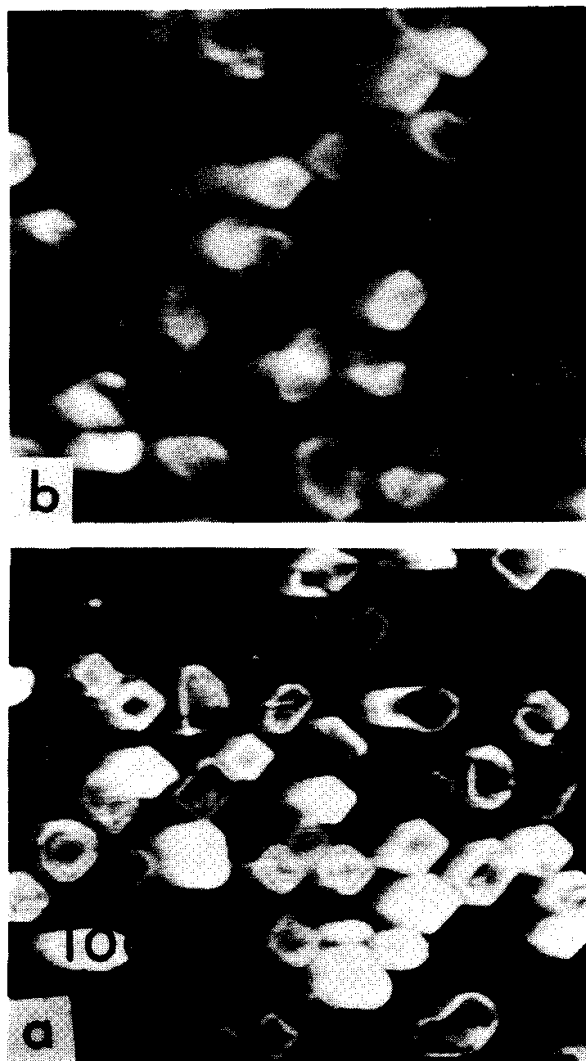


Fig. 5. Dark field images at 200 kV. (a) (200) reflection. (b) (400) reflection.

etc., along the side as in Fig. 4b. The chromatic aberration coefficient of objective lens used in this experiment was 4 mm at 50–100 kV, 4.3 mm at 200–500 kV and 5 mm at 800–1000 kV.\* Sets of images at each accelerating voltage are shown in Figs. 3–7.

### § 3. Results and Discussions

The streaks in dark field images are energy spectra of electrons due to the energy loss of incident beam in the specimen. In low accelerating voltages, when the object is small, the image formed by elastic scattering separates thoroughly from that formed by the characteristic loss electrons as shown in Fig. 8.

#### A. Images formed by elastic scattering (elastic images)

The quality of the elastic images in low

\* The pictures in this region were taken in Central Research Laboratory, Hitachi Ltd. by the generosity of Dr. B. Tadano to whom the present author is deeply grateful.

accelerating voltages are very poor. The image quality is nearly the same for (200) reflection at 50 kV, (220) at 100 kV and (400) at 200 kV as shown in Figs. 3, 4 b and 5 b. The deflecting angles, twice the Bragg angles, for these reflections at the corresponding voltages are approximately the same (see  $\times$  in Fig. 13). This implies that the image quality is mainly determined by the deflecting angle independent of the accelerating voltage. The reason for this is as follows. Since the spherical aberration may be given as  $\delta_s = C_s \alpha^3$ , where  $C_s$  is the spherical aberration coefficient and  $\alpha$  is the deflecting angle, the electrons passing the points on the segment  $AA'$  and those passing the points on the segment  $BB'$  focus approximately on the plane  $F'$  and  $F''$ , respectively as shown in Fig. 9. The focal line on the plane  $F''$  is vertical to the plane of the figure and that on  $F'$  is parallel to it. The circle of minimum confusion is formed on  $\bar{F}$ . Thus, although the electron microscope is adjusted to exclude the astigmatism under bright field, the images under dark field become apparently astigmatic due to the spherical aberration. The astigmatic difference turns out to be  $\Delta f_A = 2C_s \alpha^2 M^2$ , where  $M$  is the magnification. The length of the focal lines on  $F'$  and  $F''$  is  $4C_s \alpha^2 \delta \alpha M$ , where  $\delta \alpha$  is the angle corresponding to the radius of the diffraction spot and is smaller than the half angle of the objective lens aperture. The diameter of the minimum confusion circle due to the apparent astigmatism is  $d_{\min} = 2C_s \alpha^2 \delta \alpha$  which limits the resolution of the elastic images. This shows that the resolution is mainly determined by the deflecting angle independent of the accelerating voltage, because  $C_s$  and  $\delta \alpha$  vary only slowly with it. If it is assumed, according to the experimental conditions of Fig. 3, 4 b and 5 b, that  $C_s = 5$  mm,  $\alpha = 2.5 \times 10^{-2}$  rad and  $\delta \alpha = 1 \times 10^{-3}$  rad,  $d_{\min}$  turns out to be about 60 Å. This is in accord with the experimental result.

When the reflection order is fixed, the deflecting angle  $\alpha$  decreases in proportion to the wavelength. Thus the resolution, the reciprocal of the minimum confusion circle, is improved more quickly than in proportion to the accelerating voltage. An improvement for the reflection (400), for example, is shown

in Fig. 5 b (200 kV), 6 b (500 kV) and 7 b (800 kV).

B. Images formed by inelastic scattering (inelastic image)

The image formed by the characteristic loss is seen in the continuous streak as seen in Fig. 8. The shift of this image from the corresponding elastic image is denoted by  $l_c$ . The length of the streak was roughly estimated from plates of adequate exposures and is denoted by  $l_s$ .

When the accelerating voltage was fixed and the reflection order was changed,  $l_c$  and  $l_s$  changed in proportion to the deflecting angle. The result for 100 kV, for example, is shown in Fig. 10.

The characteristic loss value of gold was determined from the known value 25 volt<sup>3)</sup> of MgO by comparing  $l_c$  of gold with that of MgO in (200) reflection at 100 kV. The value for gold was found to be 25 volt in agreement with the value of Watanabe.<sup>4)</sup>

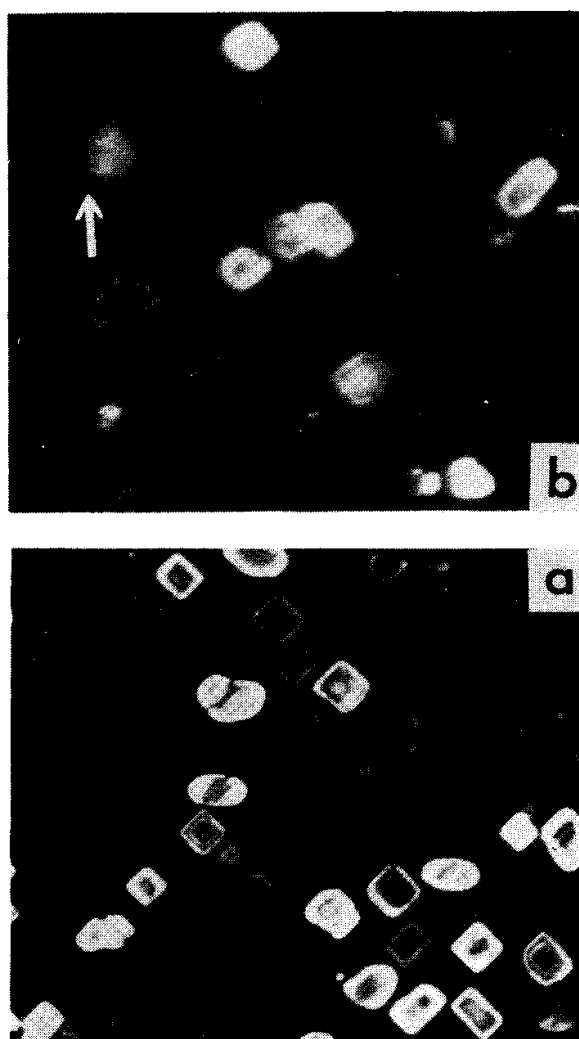


Fig. 6. Dark field images at 500 kV. (a) (200) reflection. (b) (400) reflection. The arrow shows double image due to elastic scattering and characteristic loss.

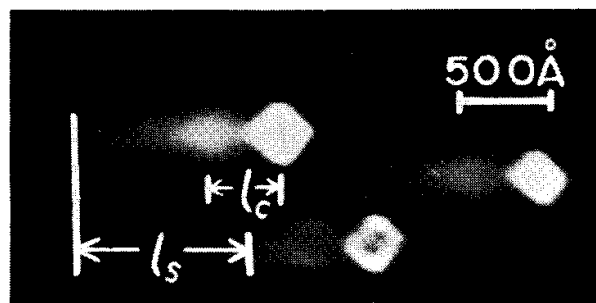


Fig. 8. Dark field image at 100 kV, (200) reflection. The arrow shows the image due to the characteristic loss.  $l_c$  is the shift due to the characteristic loss and  $l_s$  is the length of the streak.

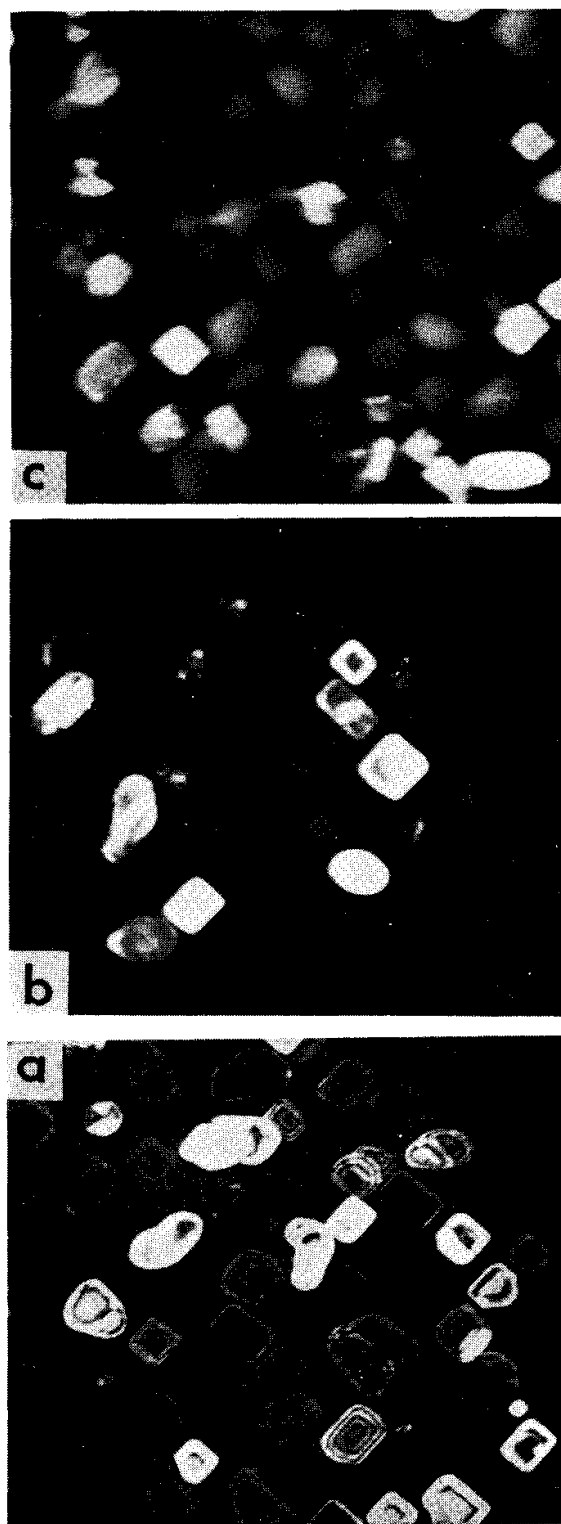


Fig. 7. Dark field images at 800 kV. (a) (200) reflection. (b) (400) reflection. (c) (600) reflection.

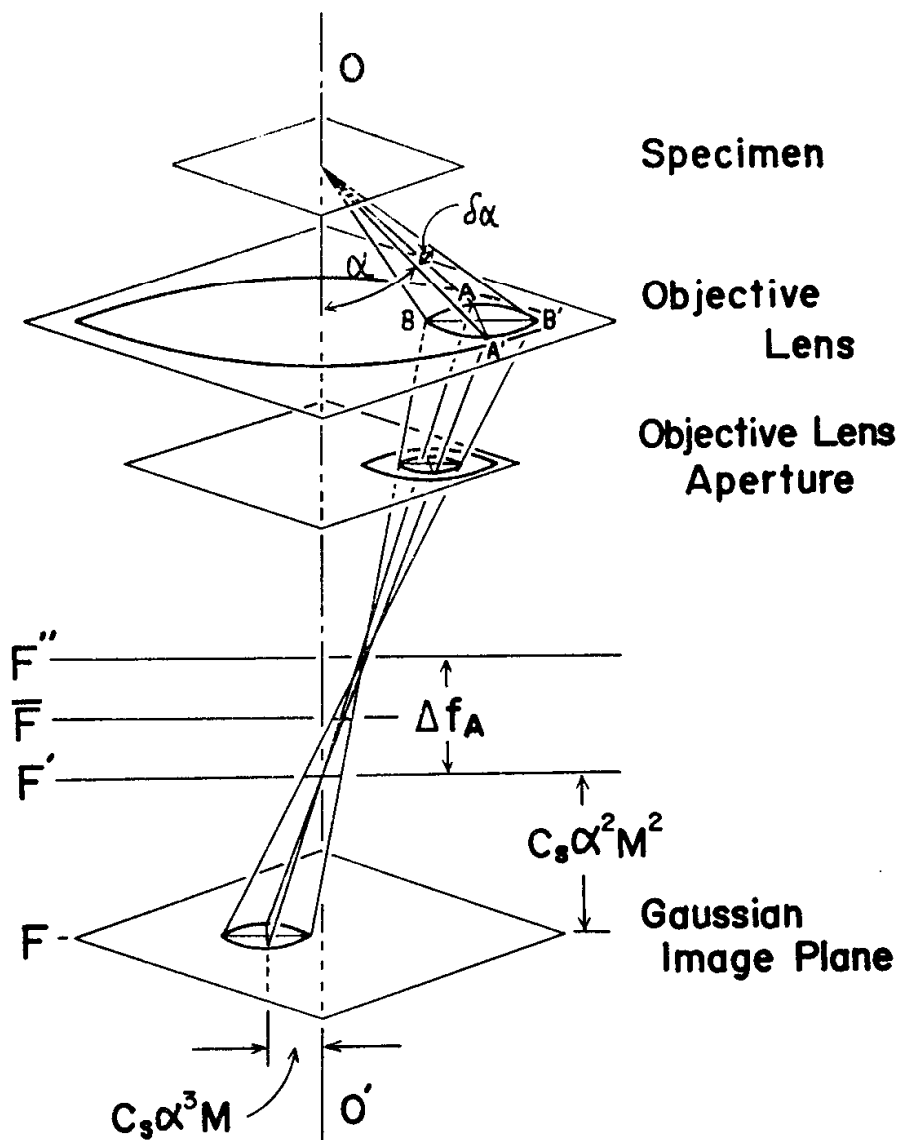


Fig. 9. The astigmatism due to the spherical aberration. The optic axis is shown by  $OO'$ . The shift due to the spherical aberration on Gauss Plane is shown by  $\delta_s M$ .

The variation of  $l_o$  and  $l_s$  in (200)-images with the accelerating voltage was investigated.  $l_o$  and  $l_s$  were large and measured easily in voltages lower than 200 kV. They became quickly small with increasing accelerating voltages. Since  $l_o$  and  $l_s$  of (200)-images were too small to measure at voltages higher than 500 kV, they were calculated from those measured for higher order reflections, assuming that  $l_o$  and  $l_s$  are proportional to  $\alpha$ . At 500 kV, in (400)-images, double images due to  $l_o$  were often observed and  $l_o$  and  $l_s$  were nearly the same. The quality of (600)-images at 800 kV was nearly the same as that of (400)-images at 500 kV (Fig. 7 c and 6 b). At 1000 kV, in (400)-images,  $l_o$  and  $l_s$  could not be measured. The experimental values of  $l_o$  and  $l_s$  are shown by marks  $\circ$  and  $\bullet$ , respectively in Fig. 11.

Theoretically, the chromatic aberration due

to energy loss may be given as  $\delta_o = C_o \gamma (\Delta E/E) \alpha$  where  $C_o$  is the chromatic aberration coefficient,  $\Delta E$  is the energy loss in the specimen,  $E$  is the accelerating voltage and the relativistic term  $\gamma$  is given as  $\gamma = \{1 + eE/(mc^2)\} / \{1 + eE/(2mc^2)\}$ .<sup>51</sup> Using the wavelength  $\lambda$  and the spacing  $d_{hkl}$  of a reflecting plane ( $hkl$ ),  $\alpha$  is given approximately as  $\lambda/d_{hkl}$ . When the energy loss  $\Delta E$  is the characteristic loss,  $\Delta E$  is a constant,  $\Delta E = 25$  volt, independent of  $E$ . Thus  $l_o$  can be calculated from the formula  $l_o = 6.3 \times 10^8 \gamma \lambda / E \text{ \AA}$  by taking  $C_o = 5$  mm and  $d_{200} = 2 \text{ \AA}$ . The variation of  $l_o$  with the accelerating voltage is drawn by the solid curve in Fig. 11. The curve is in accord with the experimental results at voltages lower than 500 kV. The experimental value  $C_o = 5$  mm is a little larger than the value for the objective lens  $C_o = 4 \sim 5$  mm (see § 2). The difference at lower

voltages may be due to the chromatic aberration of the intermediate lens. The experimental results of the length of streaks  $l_s$  are plotted by the dotted curve in Fig. 11,

although they cannot be measured exactly. The empirical curve for  $l_s$  drops more quickly with the accelerating voltage than that of  $l_c$ . The empirical curve shown by the dotted line is drawn by taking  $l_s = 4.8 \times 10^8 \gamma \lambda / (E\beta^2)$ ,

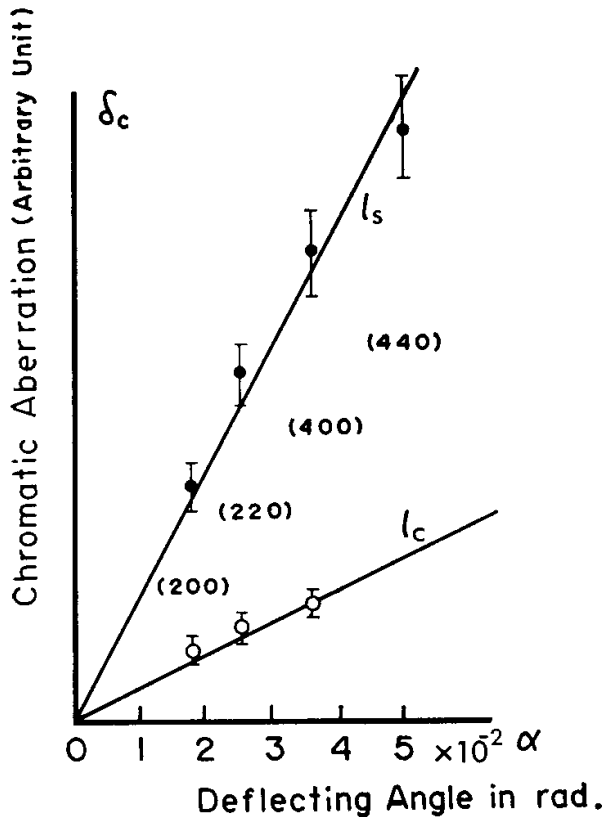


Fig. 10. Experimental value at 100 kV of chromatic aberration plotted against the deflecting angle.  $\circ$  and  $\bullet$  indicate  $l_c$  and  $l_s$ , respectively.

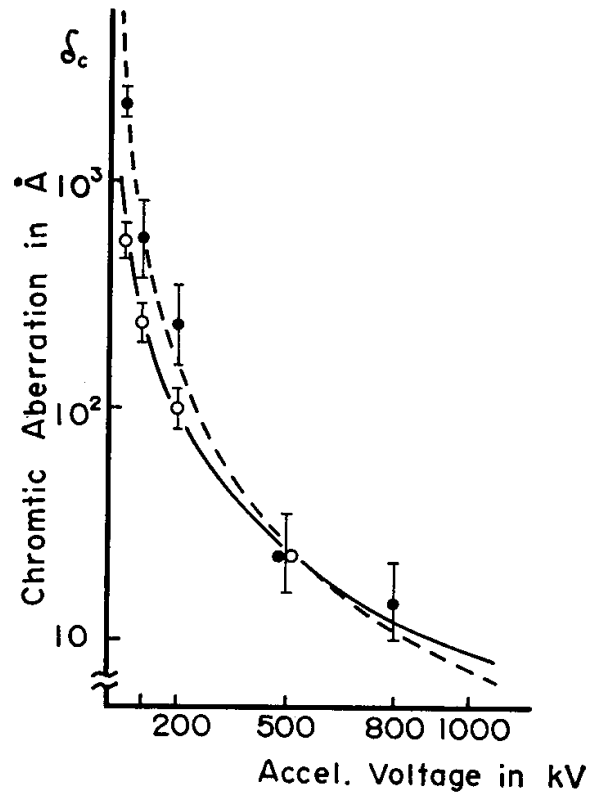


Fig. 11. The chromatic aberrations in (200)-images plotted against the accelerating voltage.  $\circ$  and  $\bullet$  indicate  $l_c$  and  $l_s$ , respectively.

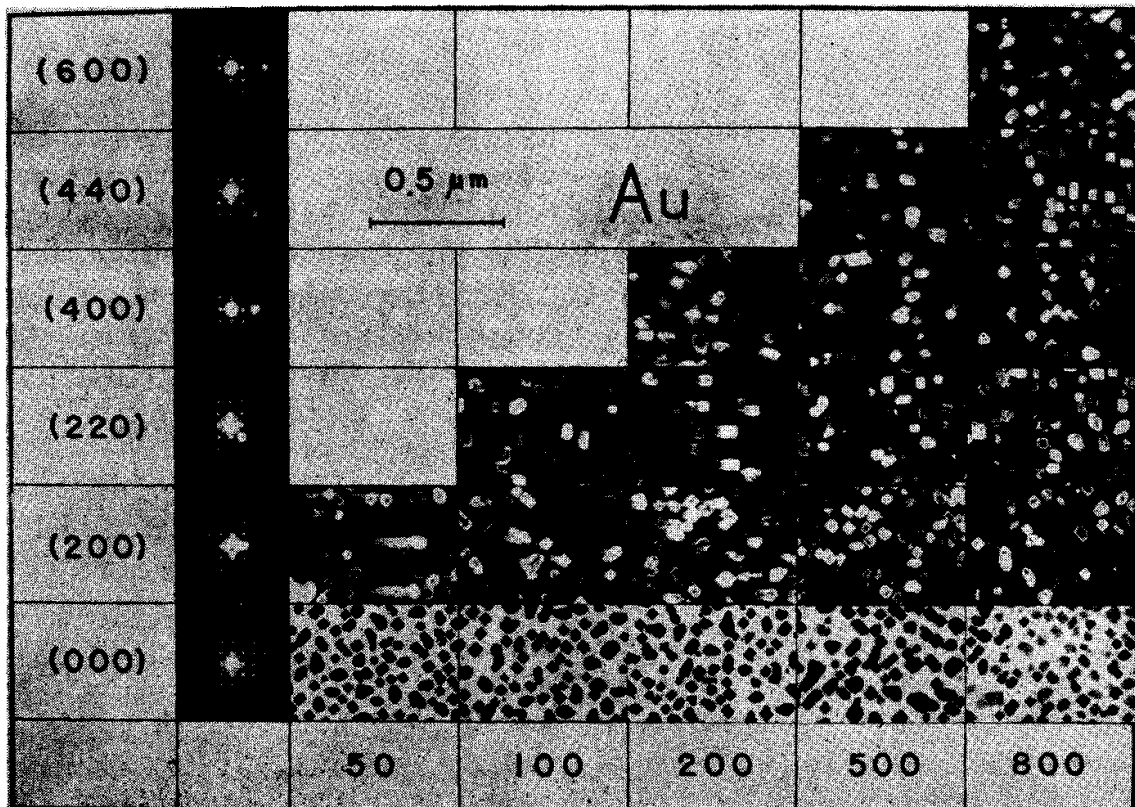


Fig. 12. Bright and dark field images taken at various accelerating voltages. Abscissa is accelerating voltage in kV and ordinate, index of reflection.